Sensors and Actuators B 155 (2011) 782–788

Contents lists available at ScienceDirect

Sensors and Actuators B: Chemical

journal homepage: www.elsevier.com/locate/snb

Improved selective acetone sensing properties of Co-doped ZnO nanofibers by electrospinning

Li Liu[a,*], Shouchun Li[a], Juan Zhuang[b], Lianyuan Wang[a], Jinbao Zhang[a], Haiying Li[a], Zhen Liu[a], Yu Han[a], Xiaoxue Jiang[c], Peng Zhang[c]

[a] State Key Laboratory of Superhard Materials, College of Physics, Jilin University, Qianjing Street 2699#, Changchun 130012, PR China
[b] School of Physics and Optoelectronic Engineering, Dalian University of Technology, Dalian 116024, PR China
[c] College of Instrumentation & Electrical Engineering, Jilin University, Changchun 130012, PR China

ARTICLE INFO

Article history:
Received 29 August 2010
Received in revised form 24 January 2011
Accepted 26 January 2011
Available online 1 March 2011

Keywords:
ZnO
Semiconductors
Electrospinning
Nanofibers
Gas sensors

ABSTRACT

Pure and Co-doped (0.3 wt%, 0.5 wt%, and 1 wt%) ZnO nanofibers are synthesized by an electrospinning method and followed by calcination. The as-synthesized nanofibers are characterized by X-ray powder diffraction (XRD), scanning electron microscopy (SEM), transmission electron microscopy (TEM), and energy dispersive X-ray (EDX) spectroscopy. Comparing with pure ZnO nanofibers, Co-doped nanofibers exhibit improved acetone sensing properties at 360 °C. The response of 0.5 wt% Co-doped ZnO nanofibers to 100 ppm acetone is about 16, which is 3.5 times larger than that of pure nanofibers (about 4.4). The response and recovery times of 0.5 wt% Co-doped ZnO nanofibers to 100 ppm acetone are about 6 and 4 s, respectively. Moreover, Co-doped ZnO nanofibers can successfully distinguish acetone and ethanol/methanol, even in a complicated ambience. The high response and quick response/recovery are based on the one-dimensional nanostructure of ZnO nanofibers combining with the Co-doping effect. The selectivity is explained by the different optimized operating temperatures of Co-doped ZnO nanofibers to different gases.

1. Introduction

ZnO, a II–VI compound semiconductor, has found a multitude of applications as a result of its wide and direct band gap, high exciton binding energy at room temperature, appropriate resistivity for peripheral circuits, ease of fabrication, and good safety record [1–3]. It has been extensively studied for catalysis [4], field-emission devices [5], optoelectronics [5], and chemical sensors [6]. In the sensor field, ZnO has been proved to be a highly sensitive material for the detection of both reducing and oxidizing gases [7]. Many scientific and technological efforts have been made to improve its response, reaction speed, selectivity, and stability [8–11]. In recent years, interest in one-dimensional (1D) ZnO nanostructures has been greatly stimulated since their sensing properties can be efficiently enhanced in this way. The high surface-to-volume ratio of these 1D ZnO nanostructures (a higher surface area provides more sites for analyte molecules adsorption) make them much sensitive than ZnO nanoparticles and thin films [12]. Hitherto, 1D ZnO nanostructures with different morphologies have been successfully developed including nanorods [12,13], nanotubes [14], nanowires [15], nanobelts [16,17], and nanofibers [18]. The gas sensing investigation reveals that these nanostructures hold high response to H_2, CO, NO, H_2O, and ethanol [12–18]. However, to the best of our knowledge, rare investigations concern the acetone sensing characteristics of 1D ZnO nanostructures.

Electrospinning is a unique technique which offers a relatively facile and versatile method for the large-scale synthesis of 1D nanostructures that are exceptionally long in length, uniform in diameter, large in surface area, especially diversified in composition [19–22]. Our group has successfully synthesized several semiconductor nanofibers with different gas or humidity sensing properties by electrospinning [18,20,23]. In this paper, promoted by both the distinct properties of 1D nanostructure and the effects of metal additives on the sensing performance, we develop an in situ process for sensitizing ZnO by adding cobaltous nitrate during electrospinning and subsequent calcination. Co-doped ZnO nanofibers exhibit high sensitivity and quick response/recovery to acetone. And this material also shows the successful discrimination between acetone and ethanol/methanol, which makes it a good candidate in fabricating highly selective sensors in practice.

2. Experimental

2.1. Preparation and characterization of materials

Zinc nitrate, cobaltous nitrate and poly (viny pyrroridone) (PVP, M_W = 1,300,000) were supplied by Beijing Chemical Co. (China).

* Corresponding author. Tel.: +86 431 8502260; fax: +86 431 8502260.
E-mail address: liwei99@jlu.edu.cn (L. Liu).

0925-4005/$ – see front matter © 2011 Elsevier B.V. All rights reserved.
doi:10.1016/j.snb.2011.01.047

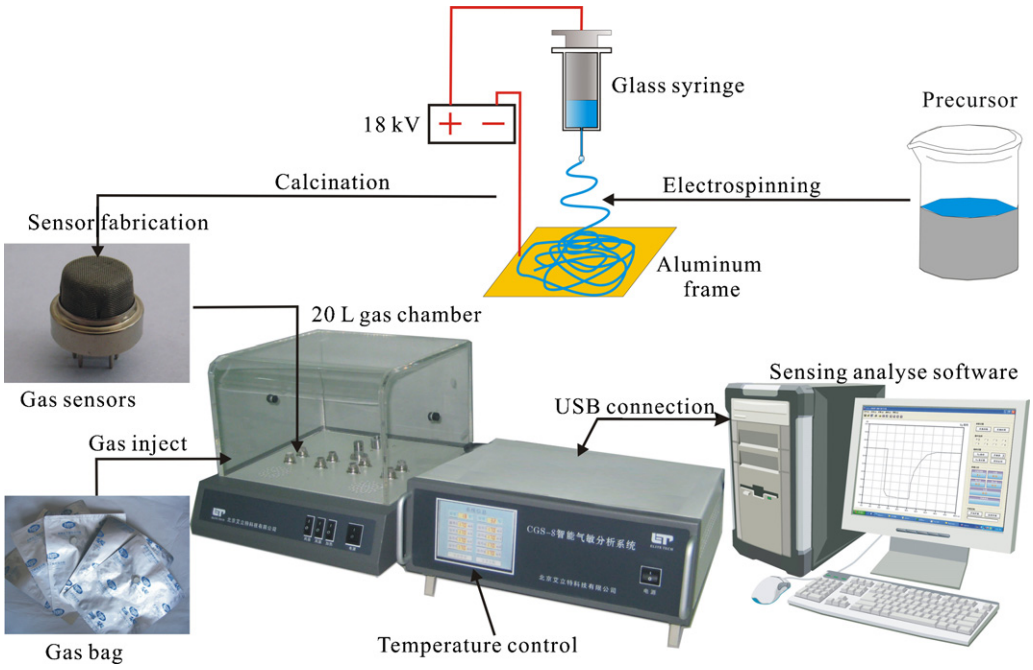

Fig. 1. Schematic diagram of the experimental apparatus.

Ethanol and N,N-dimethylformamide (DMF) were bought from Tianjin Tiantai Chemical Co. (China). All the chemicals were analytical grade and used as received without further purification.

Co-doped ZnO nanofibers were synthesized by an electrospinning method and followed by calcination. In a typical procedure, 0.595 g of zinc nitrate and certain amount of cobaltous nitrate (0, 0.3 wt%, 0.5 wt%, and 1 wt%) were added into a solvent of DMF in a glove box under vigorous stirring for 6 h. Subsequently, 1 g of PVP was dissolved into 8 mL ethanol in another glove box under vigorous stirring for 6 h. Then, both of them were mixed together under stirring and then loaded into a glass syringe for electrospinning by applying a high voltage of 18 kV at an electrode distance of 20 cm. The composite nanofibers were collected on an aluminum frame, transferred to a standard microscopic thin mica slide. After that, the organic constituents were selectively removed from these nanofibers by calcining them at 500 °C for 5 h, and crystal nanofibers were obtained.

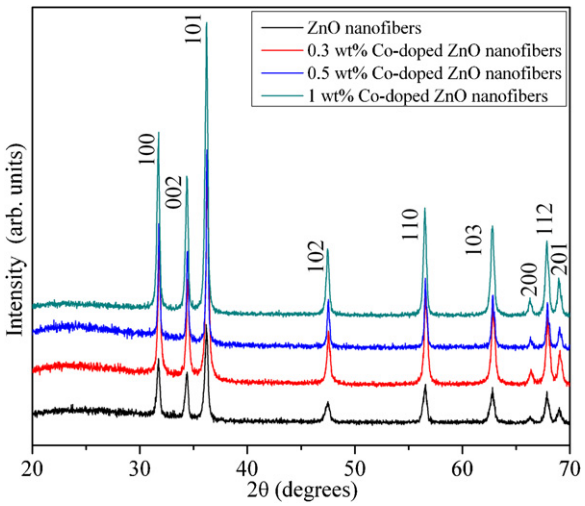

Fig. 2. XRD patterns of pure, 0.3 wt%, 0.5 wt%, and 1 wt% Co-doped ZnO nanofibers.

The crystal structures of the products were determined by X-ray powder diffraction (XRD) using an X-ray diffractometer (Siemens D5005, Munich, Germany) with Cu Kα radiation (λ = 1.5418 Å). The morphologies of the electrospun nanofibers were viewed by scanning electron microscopy (SEM, SSX-550, Shimadzu equipped with energy dispersive X-ray (EDX) spectroscopy). Transmission electron microscopy (TEM, Model JEM-2000EX, JEOL) was performed with an accelerating voltage of 200 kV.

2.2. Fabrication and measurement of sensors

The as-calcined sample was mixed with deionized water (resistivity = 18.0 MΩ cm^{-1}) in a weight ratio of 100:20 to form a paste. The paste was coated on a ceramic tube on which a pair of gold electrodes was previously printed, and then a Ni–Cr heating wire was inserted in the tube to form a side-heated gas sensor (Fig. 1) [24]. The thickness of the sensing films was measured to be about 300 μm.

Gas sensing properties were measured by a CGS-8 (Chemical gas sensor-8) intelligent gas sensing analysis system (Beijing Elite Tech Co., Ltd., China) (Fig. 1) [25]. The sensors were pre-heated at different operating temperatures for about 30 min. When the resistances of all the sensors were stable, saturated target gas was injected into the test chamber (20 L in volume) by a micro-injector through a rubber plug. The saturated target gas was mixed with air (relative humidity was about 25%) by two fans in the analysis system. After the sensor resistances reached a new constant value, the test chamber was opened to recover the sensors in air. All the measurements were performed in a laboratory fume hood. The sensor resistance and response values were acquired by the analysis system automatically. The whole experiment process was performed in a super-clean room with the constant humidity and temperature (which were monitored by the analysis system).

The response value (R) was defined as $R = Ra/Rg$, where Ra was the sensor resistance in air (base resistance) and Rg was a mixture of target gas and air. The time taken by the sensor to achieve 90% of the total resistance change was defined as the response time in the case of response (target gas adsorption) or the recovery time in the case of recovery (target gas desorption).

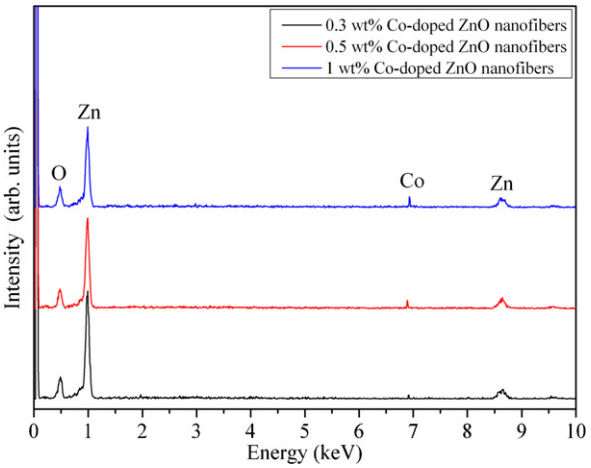

Fig. 3. EDX patterns of 0.3 wt%, 0.5 wt%, and 1 wt% Co-doped ZnO nanofibers.

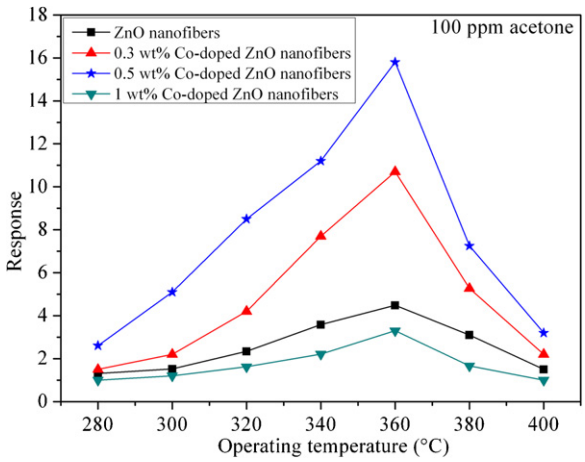

Fig. 5. Responses of pure, 0.3 wt%, 0.5 wt%, and 1 wt% Co-doped ZnO nanofibers to 100 ppm acetone at different temperatures.

3. Results and discussion

Fig. 2 shows the XRD patterns of pure, 0.3 wt%, 0.5 wt%, and 1 wt% Co-doped ZnO nanofibers. The samples are polycrystalline in nature. All the diffraction peaks can be indexed as hexagonal ZnO with lattice constants $a = 3.25$ Å and $c = 5.21$ Å, which are consistent with the values in the standard card (Joint Committee for Powder Diffraction Studies (JCPDS) card # 36-1451). For Co-doped ZnO nanofibers, the peak position of the wurtzite structure peaks shifts to higher angles compared with pure ZnO, but this tendency is not very obvious because of just a little difference in ionic radius of Zn^{2+} (0.74 Å), Co^{2+} (0.74 Å) and Co^{3+} (0.63 Å) ions.

The EDX patterns of Co-doped ZnO nanofibers in Fig. 3 indicate that the as-prepared nanofibers are composed of ZnO, O, and Co.

Fig. 4 shows the SEM images of the as-prepared nanofibers with different Co doping rates. It can be clearly seen that the diameters of the products become thinner by Co-doping. This is because the charges (Co^{+} and NO_3^{-}) added during the electrospinning will make the fibers thinner [26]. The average diameters of pure, 0.3 wt%, 0.5 wt%, and 1 wt% Co-doped ZnO nanofibers are about 180, 100, 80, and 85 nm, respectively. Feature of the 0.5 wt% Co-doped ZnO nanofibers were examined by TEM (insert in Fig. 4(c)), which shows a typical characteristic of the nanofibers.

Gas sensing experiments were performed at different temperatures to find out the optimum operating condition for acetone detection. Fig. 5 shows the responses of pure, 0.3 wt%, 0.5 wt%, and 1 wt% Co-doped ZnO nanofibers to 100 ppm acetone at different operating temperatures. The responses of all samples are found to increase with increasing the operating temperature, which attain the maximum at 360 °C, and then decrease with a further rise of the operating temperature. This behavior can be explained from the kinetics and mechanics of gas adsorption and desorption on the surface of ZnO or similar semiconducting metal oxides [27–29]. When the operating temperature is too low, the chemical activa-

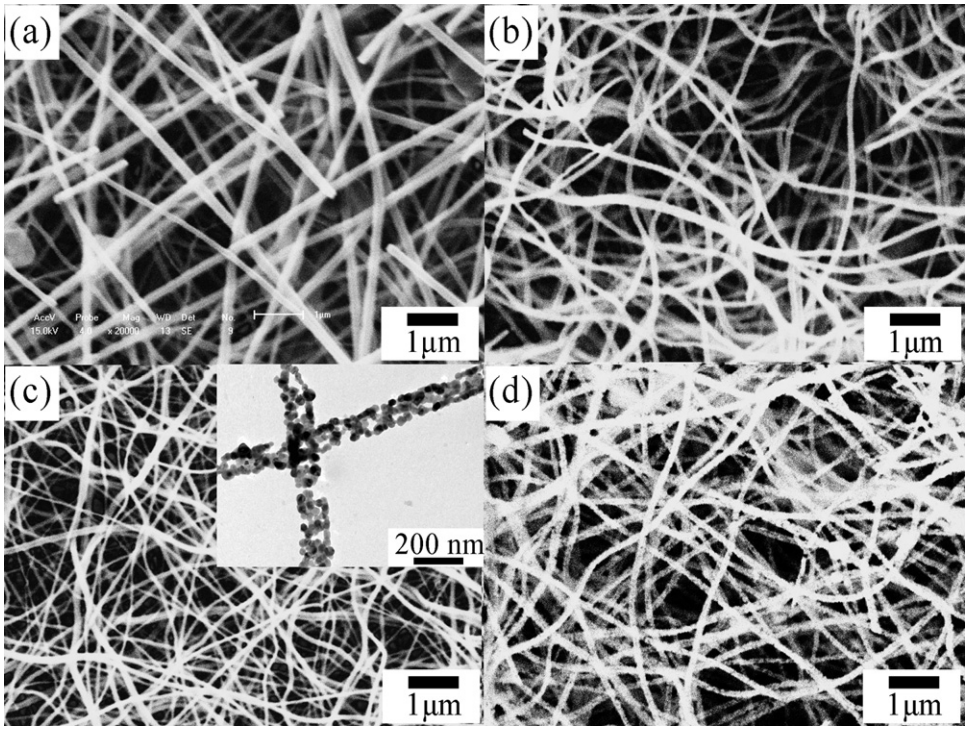

Fig. 4. SEM images of (a) pure, (b) 0.3 wt%, (c) 0.5 wt% (the insert shows a corresponding TEM image), and (d) 1 wt% Co-doped ZnO nanofibers.

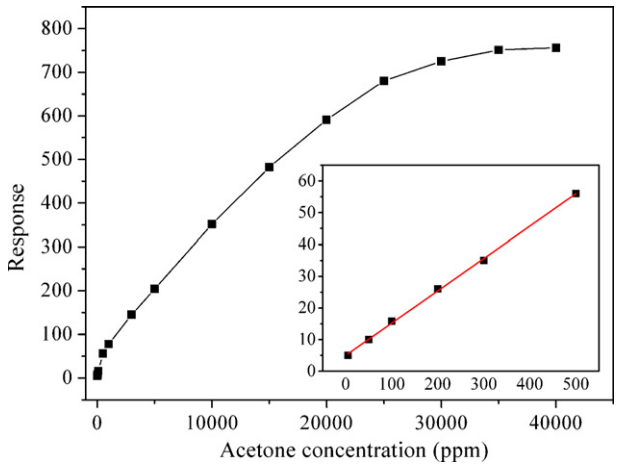

Fig. 6. Responses of 0.5 wt% Co-doped ZnO nanofibers to different concentrations of acetone at 360 °C, the insert shows the calibration curve in the range of 5–500 ppm.

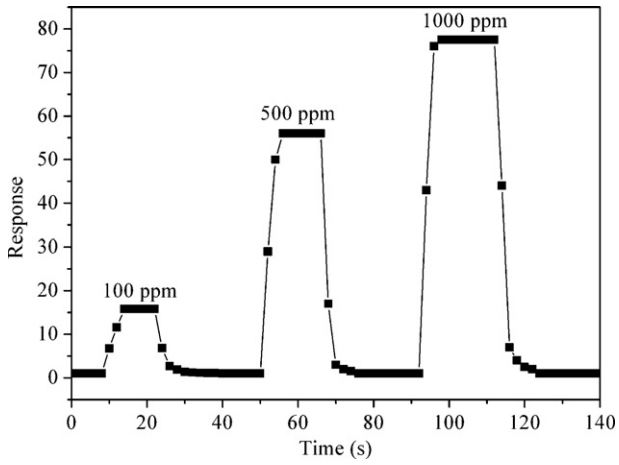

Fig. 7. Response versus time curves of 0.5 wt% Co-doped ZnO nanofibers to 100, 500, and 1000 ppm acetone consecutively at 360 °C.

tion of nanofibers is consequently small, leading to a very small response. When the operating temperature increased too much, some adsorbed gas molecules may escape before their reaction due to their enhanced activation, thus the response will decrease correspondingly. At the optimal temperature of 360 °C (corresponding to the maximum response), 0.5 wt% Co-doped ZnO nanofibers exhibit the highest response values (16), which is 3.5 times larger than that of pure nanofibers (4.4). Thus this sample is applied in the entire investigations hereafter. The base resistances (Ra) of the sensors based on pure, 0.3 wt%, 0.5 wt%, and 1 wt% Co-doped ZnO nanofibers are about 1.3, 1.8, 1.6, and 9.7 MΩ, respectively.

Fig. 6 shows the sensor response versus acetone concentration at 360 °C. The sensor can detect acetone down to 5 ppm (the corresponding response is about 5). In the range of 5–500 ppm, the response linearly increases with increasing the acetone concentration (insert in Fig. 6). Above 500 ppm, the response slowly increases, which indicates that the sensor becomes more or less saturated. Finally the sensor reaches saturation at about 35,000 ppm. In fact, the response of the semiconducting oxide gas sensitive sensor can usually be empirically represented as $R = A[C]^N + B$ [30–32], where A and B are constants and $[C]$ is the concentration of the target gas. N usually has a value between 0.5 and 1.0, depending on the charge of the surface species and the stoichiometry of the elementary reactions on the surface. For the Co-doped ZnO nanofibers, N is around 1 for acetone in the range of 5–500 ppm at 360 °C. Such a linear dependence indicates that these nanofibers can be used as promising materials for acetone sensors.

The response versus time curves of 0.5 wt% Co-doped ZnO nanofibers to different concentrations of acetone are shown in Fig. 7. For acetone at levels of 100, 500 and 1000 ppm, the responses are about 16, 56 and 77.5, respectively. The response time and recovery time are about 6 and 4 s, respectively for the sensor to 100 ppm acetone. With the increase in acetone concentration, the response time decreases gradually. The response times are calculated to be about 5 s for 500 ppm acetone and 4 s for 1000 ppm acetone. The decrease in response time can be explained by the varieties of the saturation time and mean residence period of the acetone molecules on the film surface. When the acetone concentration is low, the time required for the complete reaction of the oxygen species and acetone molecules is long, leading to long response time. As the concentration increases, the reaction time decreases, and the response time decreases accordingly. No obvious change in recovery time can be found in our experiment, which may due to the high operating temperature of the sensors. Moreover, constant base resistance (Ra) has also been realized among the consecutive tests, which demonstrates the chemical stability of the Co-doped ZnO nanofibers.

The sensor selectivity was tested by exposing it to 100 ppm different gases (including a mixture gas of 100 ppm acetone and 100 ppm ethanol) at 360 °C. As shown in Fig. 8, the sensor response to acetone (CH_3COCH_3) is much higher than that to ethanol (C_2H_5OH), methanol (CH_3OH), toluene (C_6H_5OH), H_2, NH_3, C_6H_6, CH_4, and CO. Especially, the response to acetone (16) is almost 4 times larger than to ethanol (4.1) and 5 times larger than to methanol (3.4), and is only about 17.5 to the mixture gas of 100 ppm acetone and 100 ppm ethanol. These results indicate 0.5 wt% Co-doped ZnO nanofibers can successfully distinguish acetone and ethanol/methanol.

To further know the selectivity of 0.5 wt% Co-doped ZnO nanofibers, the sensor was also exposed to different concentrations of acetone, ethanol, and methanol at 360 °C (Fig. 9). The distinction between the responses to acetone and to ethanol/methanol is found to increase by increasing the gas concentrations. At the saturated concentration for acetone (about 35,000 ppm), the response to acetone is about 7 times larger than to ethanol or methanol. The results suggest that better selectivity can be achieved at higher gas concentrations.

To test the fiber selectivity in practice, we prepared a complicated gas by mixing 100 ppm C_6H_5OH, H_2, NH_3, C_6H_6, CH_4, and CO as the background ambience, and then injected acetone, ethanol, and methanol, respectively. The results shown in Fig. 10 exhibit that 0.5 wt% Co-doped ZnO nanofibers can distinguish acetone and

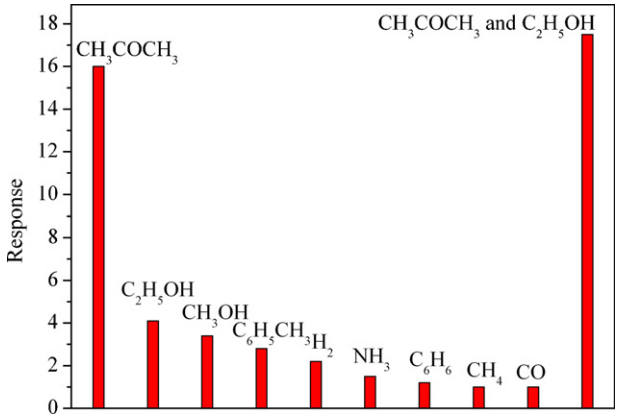

Fig. 8. Responses of 0.5 wt% Co-doped ZnO nanofibers to 100 ppm different gases at 360 °C.

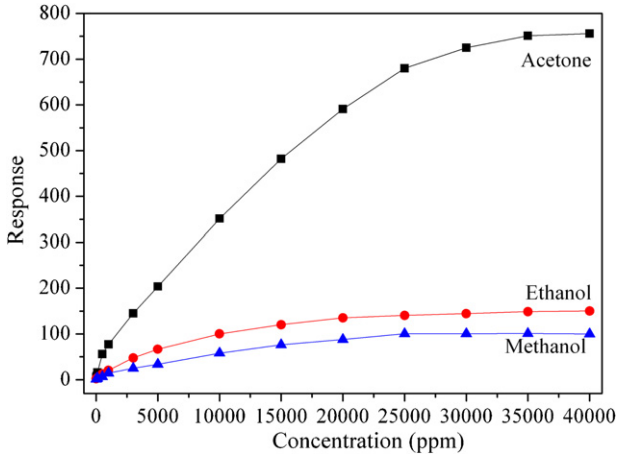

Fig. 9. Responses of 0.5 wt% Co-doped ZnO nanofibers to different concentrations of acetone, ethanol, and methanol at 360 °C.

ethanol/methanol in this mixed gas ambience. The results are based on the much higher response values of 0.5 wt% Co-doped ZnO nanofibers to acetone than to other gases. Thus the sensor exhibits prominently and highly selective, and can be put into various practical applications.

There have been many studies on various sensor materials for detecting acetone, ethanol, and methanol. However, the sensing behavior to these three gases are similar in most investigations, and the cross sensitivity among them cannot be avoided [33–36]. In our case, the sensor presents successful discrimination between acetone and ethanol/methanol, which may be due to the different optimized operating temperature for this sensor to these three gases. As can be seen in Fig. 11, the maximum response values appear at 300 °C for the sensor to ethanol, and at 320 °C to methanol. At 320 °C, the responses to acetone, ethanol, and methanol are very close. And the sensor instead exhibits higher response to ethanol than to acetone at 300 °C.

To reveal the Co effect on the selectivity performance of ZnO nanofibers, we also tested the responses of pure ZnO nanofibers to 100 ppm ethanol and acetone at different temperatures (Fig. 12). The pure ZnO nanofibers exhibit the maximum response value at 340 °C to ethanol and at 360 °C to acetone, and the corresponding response values are 6 and 4.48, respectively. The results suggest that the improved selectivity of Co-doped ZnO nanofibers can be attributed to the reduced optimum operating temperatures for ethanol detection brought by appropriate Co in ZnO nanofibers.

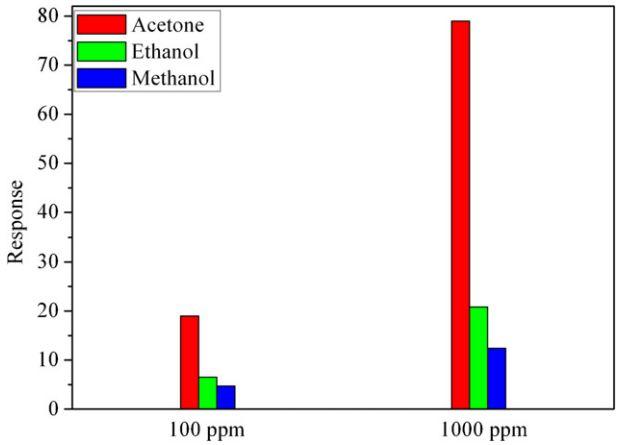

Fig. 10. Responses of 0.5 wt% Co-doped ZnO nanofibers to acetone, ethanol, and methanol in the mixed gas ambience at 360 °C.

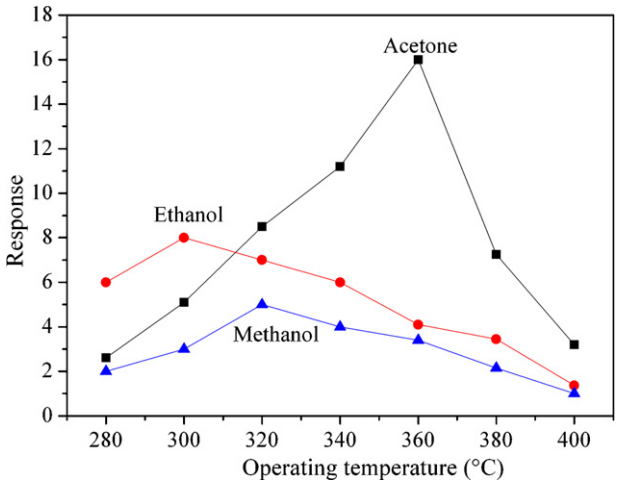

Fig. 11. Responses of 0.5 wt% Co-doped ZnO nanofibers to 100 ppm acetone, ethanol, and methanol at different operating temperatures.

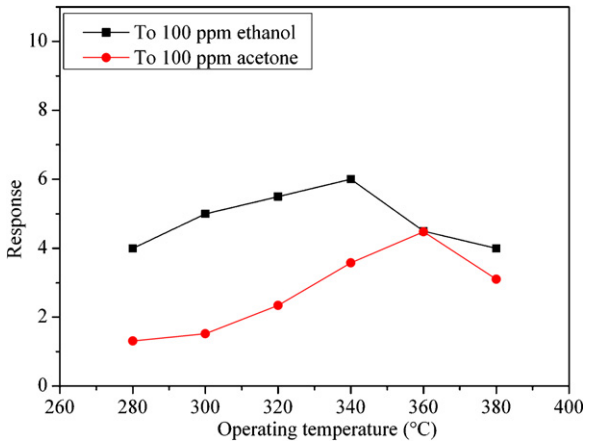

Fig. 12. Responses of pure ZnO nanofibers to 100 ppm ethanol and acetone at different temperatures.

Fig. 13 shows the variations of response of four sensors fabricated from 0.5 wt% Co-doped ZnO nanofibers to 500 ppm acetone at 360 °C. All the sensors exhibit similar sensing characteristics (response values, response times, and recovery times), indicating good reproducibility of the as-synthesized nanofibers.

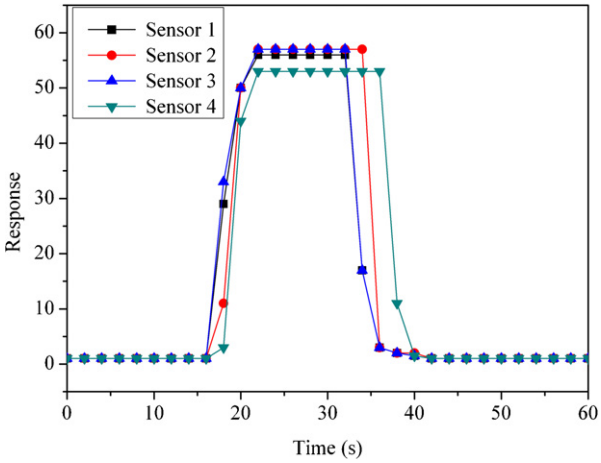

Fig. 13. Reproducibility of 0.5 wt% Co-doped ZnO nanofibers to 500 ppm acetone at 360 °C.

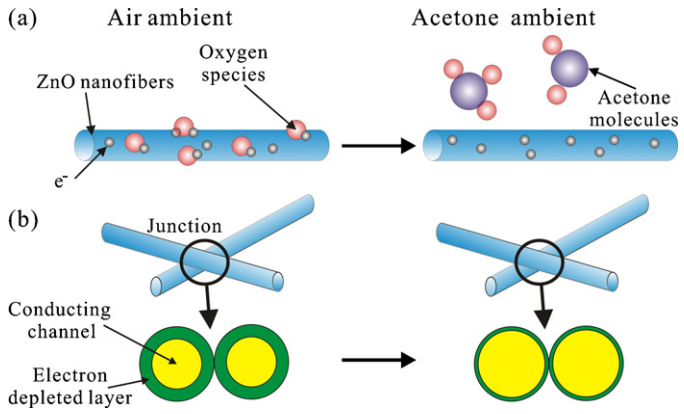

Fig. 14. Schematic diagram of ZnO nanofiber sensing mechanism.

For most semiconducting oxide gas sensor, the change in resistance is primarily caused by the adsorption and desorption of gas molecules on the surface of the sensing films [37–40,2,30]. In air ambient, ZnO nanofibers will adsorb the oxygen molecule on the surface. The adsorbed oxygen is changed into various chemical absorptive states (O^- is believed to be dominant) [41] by capturing electrons from the conductance band. This will increase the barrier height for electrons to transport and thus ZnO nanofibers will show a high resistance. When reducing gases (such as acetone in this case) are introduced, the adsorbed oxygen on ZnO nanofibers takes part in the oxidation of acetone. Once the oxidation reaction occurs, electrons could enter into the ZnO nanofibers, resulting in the decrease of sensor resistance (Fig. 14(a)).

The high response and short response/recovery times of Co-doped ZnO nanofibers are mainly based on the fiber structure. The 1D nanostructure of ZnO nanofibers possesses large surface-to-volume ratio, which is a vital factor for high sensing performance [19]. And the nanofibers synthesized by electrospinning own high length-to-diameter ratio, which may form netlike structure on the sensor surface [42]. The netlike structure will enhance the target gas adsorption, and lead to a high response value. Besides, there are many nanofiber–nanofiber junctions in the netlike structure (Fig. 14(b)). Such junctions should form a depleted layer around the intersection and block the electron flow in a way which is more efficient than the surface depletion on the individual nanofibers (contact-controlled effect) [43].

Many former papers have proved that the existence of Co in semiconductor sensing materials can improve their response prominently [44–46]. In this case, decreased fiber diameter caused by Co doping may lead to an increase of target gas adsorption, which will be resulted in the sensing improvement (shown in Fig. 4). On the other hand, Co will support the catalytic conversion of acetone into its oxidation products, which is due to spill-over of activated fragments to the semiconductor surface to react with the adsorbed oxygen and is called chemical sensitization. And this effect can accelerate the sensing reaction on the fiber surface effectively [39,47]. Furthermore, as Co_3O_4 is a p-type material [44], doping too much Co in ZnO may form Co_3O_4 (although not found in XRD pattern due to its very small amount) in ZnO nanofibers and the n-type characteristics of the ZnO will regress (corresponding to an evident increase in Ra), thus the sample with 1 wt% doping rate show a decreased response. Moreover, the improved selective sensing properties brought by Co doping can be also explained by the reduced optimum operating temperatures for ethanol detection, and the similar results are observed for many other dopants [48,49]. However, the exact mechanism for the change of the optimum operation temperature with Co doping is far more complicated and further studies are needed.

4. Conclusion

In summary, pure and Co-doped ZnO nanofibers are synthesized by an electrospinning and followed by calcination. Gas sensing investigation reveals that Co-doping can enhance the acetone sensing properties of ZnO nanofibers efficiently. Especially, Co-doped ZnO nanofibers can successfully distinguish acetone and ethanol/methanol, even in a mixed gas ambience. The high response and quick response/recovery of these nanofibers are explained by their 1D nanostructure combining with the Co-doping effect. The results demonstrate the potential application of Co-doped ZnO nanofibers for fabricating high performance acetone sensors.

Acknowledgements

This work was financially supported by the Department of Environmental Protection of Jilin Province (no. 2009-22), Jilin Provincial Science & Technology Department (no. 20100344), and The National Innovation Experiment Program for University Students (nos. 2009C65125 and 2010C65188).

References

[1] Y. Qiu, S. Yang, ZnO nanotetrapods: controlled vapor-phase synthesis and application for humidity sensing, Adv. Funct. Mater. 17 (2007) 1345–1352.
[2] X.J. Huang, Y.K. Choi, Chemical sensors based on nanostructured materials, Sens. Actuators B: Chem. 122 (2007) 659–671.
[3] B.C. Yadav, R. Srivastava, C.D. Dwivedi, P. Pramanik, Moisture sensor based on ZnO nanomaterial synthesized through oxalate route, Sens. Actuators B: Chem. 131 (2008) 216–222.
[4] C.S. Lao, P.X. Gao, R.S. Yang, Y. Zhang, Y. Dai, Z.L. Wang, Formation of double-side teethed nanocombs of ZnO and self-catalysis of Zn-terminated polar surface, Chem. Phys. Lett. 417 (2006) 358–362.
[5] J. Singh, S.S. Patil, M.A. More, D.S. Joag, R.S. Tiwari, O.N. Srivastava, Formation of aligned ZnO nanorods on self-grown ZnO template and its enhanced field emission characteristics, Appl. Surf. Sci. 256 (2010) 6157–6163.
[6] F. Boccuzzi, A. Chiorino, S. Tsubota, M. Haruta, An IR study of CO-sensing mechanism on Au/ZnO, Sens. Actuators B: Chem. 24–25 (1995) 540–543.
[7] F. Grasset, Y. Molard, S. Cordier, F. Dorson, M. Mortier, C. Perrin, M. Guilloux-Viry, T. Sasaki, H. Haneda, When "metal atom clusters" meet ZnO nanocrystals: a $((n\text{-}C_4H_9)_4N)_2Mo_6Br_{14}$@ZnO hybrid, Adv. Mater. 20 (2008) 1710–1715.
[8] R.C. Wang, H.Y. Lin, Simple fabrication and improved photoresponse of ZnO–Cu_2O core–shell heterojunction nanorod arrays, Sens. Actuators B: Chem. 149 (2010) 94–97.
[9] V. Kobrinsky, E. Fradkin, V. Lumelsky, A. Rothschild, Y. Komem, Y. Lifshitz, Tunable gas sensing properties of p- and n-doped ZnO thin films, Sens. Actuators B: Chem. 148 (2010) 379–387.
[10] I.S. Hwang, S.J. Kim, J.K. Choi, J. Choi, H. Ji, G.T. Kim, G. Cao, J.H. Lee, Synthesis and gas sensing characteristics of highly crystalline ZnO–SnO_2 core–shell nanowires, Sens. Actuators B: Chem. 148 (2010) 595–600.
[11] L.A. Patil, A.R. Bari, M.D. Shinde, V. Deo, Ultrasonically prepared nanocrystalline ZnO thin films for highly sensitive LPG sensing, Sens. Actuators B: Chem. 149 (2010) 79–86.
[12] Z.P. Sun, L. Liu, L. Zhang, D.Z. Jia, Rapid synthesis of ZnO nano-rods by one-step, room-temperature, solid-state reaction and their gas-sensing properties, Nanotechnology 17 (2006) 2266–2270.
[13] B Liu, H.C. Zeng, Hydrothermal synthesis of ZnO nanorods in the diameter regime of 50 nm, J. Am. Chem. Soc. 125 (2003) 4430–4431.
[14] W.Z. Xu, Z.Z. Ye, D.W. Ma, H.M. Lu, L.P. Zhu, B.H. Zhao, X.D. Yang, Z.Y. Xu, Quasi-aligned ZnO nanotubes grown on Si substrates, Appl. Phys. Lett. 87 (2005), 093110/1–093110/3.
[15] L. Liao, H.B. Lu, J.C. Li, C. Liu, D.J. Fu, Y.L. Liu, The sensitivity of gas sensor based on single ZnO nanowire modulated by helium ion radiation, Appl. Phys. Lett. 91 (2007), 173110/1–173110/3.
[16] Y.B. Li, Y. Bando, T. Sato, K. Kurashima, ZnO nanobelts grown on Si substrate, Appl. Phys. Lett. 81 (2002) 144–146.
[17] Z.W. Pan, Z.R. Dai, Z.L. Wang, Nanobelts of semiconducting oxides, Science 291 (2001) 1947–1949.
[18] Q. Qi, T. Zhang, S. Wang, X. Zheng, Humidity sensing properties of KCl-doped ZnO nanofibers with super-rapid response and recovery, Sens. Actuators B: Chem. 137 (2009) 649–655.
[19] A. Kolmakov, M. Moskovits, Chemical sensing and catalysis by one-dimensional metal-oxide nanostructures, Annu. Rev. Mater. Res. 34 (2004) 151–180.
[20] L. Liu, T. Zhang, Z.J. Wang, S.C. Li, Y.X. Tian, W. Li, High performance microstructure sensor based on TiO_2 nanofibers for ethanol, Chin. Phys. Lett. 26 (2009) 090701.
[21] A. Greiner, J.H. Wendorff, Electrospinning: a fascinating method for the preparation of ultrathin fibers, Angew. Chem. Int. Ed. 46 (2007) 5670–5703.

[22] S.K. Kim, S.H. Hwang, D. Chang, S. Kim, Preparation of mesoporous In_2O_3 nanofibers by electrospinning and their application as a CO gas sensor, Sens. Actuators B: Chem. 149 (2010) 28–33.
[23] L. Liu, C. Guo, S. Li, L. Wang, Q. Dong, W. Li, Improved H_2 sensing properties of Co-doped SnO_2 nanofibers, Sens. Actuators B: Chem. 150 (2010) 806–810.
[24] Y.X. Liang, Y.J. Chen, T.H. Wang, Low-resistance gas sensors fabricated from multiwalled carbon nanotubes coated with a thin tin oxide layer, Appl. Phys. Lett. 85 (2004) 666–668.
[25] H. Zhang, Z. Li, L. Liu, X. Xu, Z. Wang, W. Wang, W. Zheng, B. Dong, C. Wang, Enhancement of hydrogen monitoring properties based on Pd–SnO_2 composite nanofibers, Sens. Actuators B: Chem. 147 (2010) 111–115.
[26] H. Hou, Z. Jun, A. Reuning, A. Schaper, J.H. Wendorff, A. Greiner, Poly (*p*-xylylene) nanotubes by coating and removal of ultrathin polymer template fibers, Macromolecules 35 (2002) 2429–2431.
[27] N. Yamazoe, J. Fuchigami, M. Kishikawa, T. Seiyama, Interactions of tin oxide surface with O_2, H_2O and H_2, Surf. Sci. 86 (1979) 335–344.
[28] J. Herrán, O. Fernández-González, I. Castro-Hurtado, T. Romero, G.G. Mandayo, E. Castaño, Photoactivated solid-state gas sensor for carbon dioxide detection at room temperature, Sens. Actuators B: Chem. 149 (2010) 368–372.
[29] M. Ghasdi, H. Alamdari, CO sensitive nanocrystalline $LaCoO_3$ perovskite sensor prepared by high energy ball milling, Sens. Actuators B: Chem. 148 (2010) 478–485.
[30] Q. Wan, Q.H. Li, Y.J. Chen, T.H. Wang, X.L. He, J.P. Li, C.L. Lin, Fabrication and ethanol sensing characteristics of ZnO nanowire gas sensors, Appl. Phys. Lett. 84 (2004) 3654–3656.
[31] Y.J. Chen, X.Y. Xue, Y.G. Wang, T.H. Wang, Synthesis and ethanol sensing characteristics of single crystalline SnO_2 nanorods, Appl. Phys. Lett. 87 (2005), 233503/1–233503/3.
[32] P. Feng, X.Y. Xue, Y.G. Liu, T.H. Wang, Highly sensitive ethanol sensors based on {1 0 0}-bounded In_2O_3 nanocrystals due to face contact, Appl. Phys. Lett. 89 (2006), 243514/1–243514/3.
[33] B.L. Zhu, C.S. Xiea, W.Y. Wang, K.J. Huang, J.H. Hu, Improvement in gas sensitivity of ZnO thick film to volatile organic compounds (VOCs) by adding TiO_2, Mater. Lett. 58 (2004) 624–629.
[34] H. Gong, Y.J. Wang, S.C. Teo, L. Huang, Interaction between thin-film tin oxide gas sensor and five organic vapors, Sens. Actuators B: Chem. 54 (1999) 232–235.
[35] Z. Jie, H.L. Hua, G. Shan, Z. Hui, Z.J. Gui, Alcohols and acetone sensing properties of SnO_2 thin films deposited by dip-coating, Sens. Actuators B: Chem. 115 (2006) 460–464.
[36] K.W. Kim, P.S. Cho, S.J. Kim, J.H. Lee, C.Y. Kang, J.S. Kim, S.J. Yoon, The selective detection of C_2H_5OH using SnO_2–ZnO thin film gas sensors prepared by combinatorial solution deposition, Sens. Actuators B: Chem. 123 (2007) 318–324.
[37] Y. Shimizu, S. Kai, Y. Takao, T. Hyodo, M. Egashira, Correlation between methylmercaptan gas-sensing properties and its surface chemistry of SnO_2-based sensor materials, Sens. Actuators B: Chem. 65 (2000) 349–357.
[38] M. Egashira, N. Kanehara, Y. Shimizu, H. Iwanaga, Gas-sensing characteristics of Li^+-doped and undoped ZnO whiskers, Sens. Actuators B: Chem. 18 (1989) 349–360.
[39] M.E. Franke, T.J. Koplin, U. Simon, Metal and metal oxide nanoparticles in chemiresistors: does the nanoscale matter? Small 2 (2006) 36–50.
[40] N. Barsan, D. Koziej, U. Weimar, Metal oxide-based gas sensor research: how to? Sens. Actuators B: Chem. 121 (2007) 18–35.
[41] H. Windischmann, P. Mark, A model for the operation of a thin films tin oxide conductance modulation carbon monoxide sensor, J. Electrochem. Soc. 126 (1979) 627–630.
[42] Y. Zhang, J. Li, G. An, X. He, Highly porous SnO_2 fibers by electrospinning and oxygen plasma etching and its ethanol-sensing properties, Sens. Actuators B: Chem. 144 (2010) 43–48.
[43] P. Feng, Q. Wan, T.H. Wang, Contact-controlled sensing properties of flowerlike ZnO nanostructures, Appl. Phys. Lett. 87 (2005), 213111/1–213111/3.
[44] K.I. Choi, H.R. Kim, K.M. Kim, D. Liu, G. Cao, J.H. Lee, C_2H_5OH sensing characteristics of various Co_3O_4 nanostructures prepared by solvothermal reaction, Sens. Actuators B: Chem. 146 (2010) 40–45.
[45] R.J. Wu, J.G. Wu, M.R. Yu, T.K. Tsai, C.T. Yeh, Promotive effect of CNT on Co_3O_4–SnO_2 in a semiconductor-type CO sensor working at room temperature, Sens. Actuators B: Chem. 131 (2008) 306–312.
[46] T. Xu, H. Huang, W. Luan, Y. Qi, S. Tu, Thermoelectric carbon monoxide sensor using Co–Ce catalyst, Sens. Actuators B: Chem. 133 (2008) 70–77.
[47] M. Siemons, U. Simon, Preparation and gas sensing properties of nanocrystalline La-doped $CoTiO_3$, Sens. Actuators B: Chem. 120 (2006) 110–118.
[48] S. Shukla, P. Zhang, H.J. Cho, S. Seal, L. Ludwig, Room temperature hydrogen response kinetics of nano-micro-integrated doped tin oxide sensor, Sens. Actuators B: Chem. 120 (2007) 573–583.
[49] M. Rumyantseva, V. Kovalenko, A. Gaskov, E. Makshina, V. Yuscheko, I. Ivanova, A. Ponzoni, G. Faglia, E. Comini, Nanocomposites SnO_2/Fe_2O_3: sensor and catalytic properties, Sens. Actuators B: Chem. 118 (2006) 208–214.

Biographies

Li Liu received her Ph.D. degree in the field of microelectronics and solid state electronics in 2008 from Jilin University. She was appointed an associate professor in College of Physics, Jilin University in 2009. Now, she is interested in the field of sensing functional materials and gas sensors and humidity sensors.

Shouchun Li received his BS degree from the College of Physics, Jilin University, China in 2001.

Juan Zhuang received her MS degree from the College of Physics, Jilin University, China in 1999.

Lianyuan Wang received his MS degree from the College of microelectronics and solid state electronics, Jilin University, China in 2006.

Jinbao Zhang received his MS degree from the College of microelectronics and solid state electronics, Jilin University, China in 2003.

Haiying Li received his MS degree from the College of Physics, Jilin University, China in 2000.

Zhen Liu received his MS degree from the College of Physics, Jilin University, China in 2001.

Yu Han received his MS degree from the College of Physics, Jilin University, China in 2003.

Xiaoxue Jiang received his MS degree from the College of Physics, Jilin University, China in 2003.

Peng Zhang received his MS degree from the College of Physics, Jilin University, China in 2004.